PROCEEDINGS OF SCIENCE

New measurement of $K^+ \to \pi^+\nu\bar{\nu}$ branching ratio at the NA62 experiment

Angela Romano[a,*] **for the NA62 collaboration**[†]

[a] *University of Birmingham, UK*

E-mail: angela.romano@cern.ch

The $K^+ \to \pi^+\nu\bar{\nu}$ decay is a golden mode for flavour physics. Its branching ratio ($\mathcal{B}$) is predicted with high precision by the Standard Model to be less than 10^{-10}, and the decay is highly sensitive to new physics up to the highest mass scales. A new measurement of $\mathcal{B}(K^+ \to \pi^+\nu\bar{\nu})$ by the NA62 experiment at the CERN SPS is presented, using data collected in 2021–2022. The measurement $\mathcal{B}(K^+ \to \pi^+\nu\bar{\nu}) = \left(13.0^{+3.3}_{-3.0}\right) \times 10^{-11}$ with the combined datasets from 2016–2022 is reported, and for the first time the $K^+ \to \pi^+\nu\bar{\nu}$ decay is observed with a significance exceeding 5σ.

The European Physical Society Conference on High Energy Physics (EPS-HEP2025)
7-11 July 2025
Marseille, France

*Speaker

† A. Akmete, R. Aliberti, F. Ambrosino, R. Ammendola, B. Angelucci, A. Antonelli, G. Anzivino, R. Arcidiacono, M. U. Ashraf, T. Bache, A. Baeva, D. Baigarashev, L. Bandiera, M. Barbanera, V. Bautin, J. Bernhard, A. Biagioni, L. Bician, C. Biino, A. Bizzeti, T. Blazek, B. Bloch-Devaux, P. Boboc, V. Bonaiuto, M. Boretto, M. Bragadireanu, A. Briano Olvera, D. Britton, F. Brizioli, M.B. Brunetti, D. Bryman, F. Bucci, N. Canale, T. Capussela, J. Carmignani, A. Ceccucci, P. Cenci, M. Ceoletta, V. Cerny, C. Cerri, X. Chang, B. Checcucci, C. Chiarini, M. Cirkovic, A. Conovaloff, P. Cooper, E. Cortina Gil, M. Corvino, F. Costantini, D. Coward, P. Cretaro, G. D'Agostini, J.B. Dainton, P. Dalpiaz, H. Danielsson, B. De Martino, M. D'Errico, N. De Simone, D. Di Filippo, L. Di Lella, N. Doble, B. Döbrich, F. Duval, V. Duk, D. Emelyanov, J. Engelfried, T. Enik, N. Estrada-Tristan, V. Falaleev, R. Fantechi, V. Fascianelli, L. Federici, P. Fedeli, S. Fedotov, A. Filippi, R. Fiorenza, M. Fiorini, M. Francesconi, O. Frezza, J. Fry, J. Fu, A. Fucci, L. Fulton, E. Gamberini, L. Gatignon, G. Georgiev, S. Ghinescu, A. Gianoli, R. Giordano, M. Giorgi, S. Giudici, F. Gonnella, K. Gorshanov, E. Goudzovski, C. Graham, R. Guida, E. Gushchin, F. Hahn, H. Heath, J. Henshaw, Z. Hives, E.B. Holzer, T. Husek, O. Hutanu, D. Hutchcroft, L. Iacobuzio, E. Iacopini, E. Imbergamo, B. Jenninger, J. Jerhot, R.W. Jones, K. Kampf, V. Kekelidze, C. Kenworthy, D. Kereibay, S. Kholodenko, G. Khoriauli, A. Khotyantsev, A. Kleimenova, M. Kolesar, A. Korotkova, M. Koval, V. Kozhuharov, Z. Kucerova, Y. Kudenko, J. Kunze, V. Kurochka, V. Kurshetsov, G. Lanfranchi, G. Lamanna, E. Lari, G. Latino, P. Laycock, C. Lazzeroni, G. Lehmann Miotto, M. Lelak, M. Lenti, E. Leonardi, S. Lezki, P. Lichard, L. Litov, P. Lo Chiatto, F. Lo Cicero, R. Lollini, D. Lomidze, A. Lonardo, E. Long, P. Lubrano, M. Lupi, N. Lurkin, D. Madigozhin, I. Mannelli, A. Mapelli, F. Marchetto, R. Marchevski, S. Martellotti, P. Massarotti, K. Massri, E. Maurice, M. Medvedeva, A. Mefodev, E. Menichetti, E. Migliore, E. Minucci, M. Mirra, M. Misheva, N. Molokanova, M. Moulson, S. Movchan, Y. Mukhamejanov, A. Mukhamejanova, M. Napolitano, R. Negrello, I. Neri, F. Newson, A. Norton, M. Noy, T. Numao, V. Obraztsov, A. Okhotnikov, A. Ostankov, S. Padolski, R. Page, V. Palladino, I. Panichi, A. Parenti, C. Parkinson, E. Pedreschi, M. Pepe, M. Perrin-Terrin, L. Peruzzo, L. Petit, P. Petrov, Y. Petrov, F. Petrucci, R. Piandani, M. Piccini, J. Pinzino, L. Plini, I. Polenkevich, C. Polivka, L. Pontisso, Yu. Potrebenikov, D. Protopopescu, M. Raggi, M. Reyes Santos, K. Rodriguez Rivera, M. Romagnoni, A. Romano, I. Rosa, C. Rossi, P. Rubin, G. Ruggiero, V. Ryjov, A. Sadovskiy, N. Saduyev, S. Sakhiyev, K. Salamatin, A. Salamon, C. Sam, J. Sanders, C. Santoni, G. Saracino, F. Sargeni, J. Schubert, S. Schuchmann, V. Semenov, A. Sergi, A. Shaikhiev, V. Shang, S. Shkarovskiy, F. Simula, M. Soldani, D. Soldi, M. Sozzi, T. Spadaro, F. Spinella, A. Sturgess, V. Sugonyaev, J. Swallow, G. Tinti, A. Tomczak, S. Trilov, M. Turisini, P. Valente, T. Velas, B. Velghe, S. Venditti, P. Vicini, R. Volpe, M. Vormstein, H. Wahl, R. Wanke, V. Wong, B. Wrona, O. Yushchenko, M. Zamkovsky, A. Zinchenko.

https://pos.sissa.it/

PoS(EPS-HEP2025)299

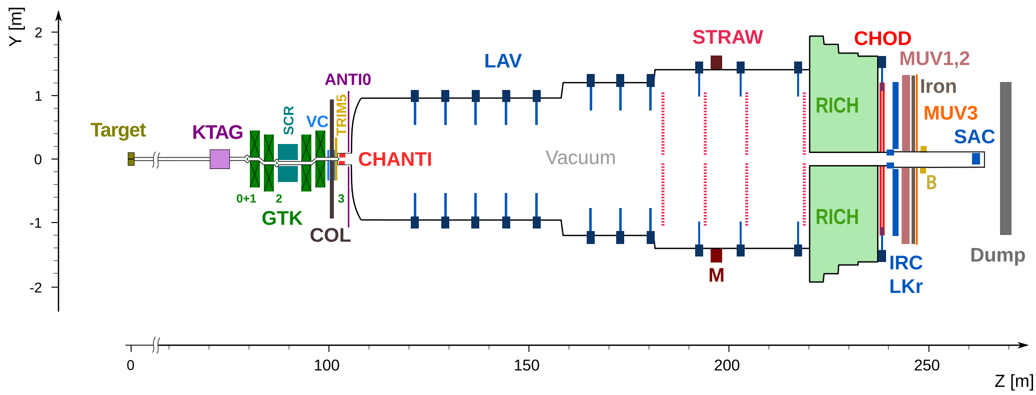

Figure 1: Schematic side view of the NA62 detector for data-taking from 2021 onwards.

1. Introduction

The $K \to \pi\nu\bar{\nu}$ decays are Flavour Changing Neutral Current (FCNC) processes and are therefore of particular interest in the study of flavour physics. In the Standard Model (SM), these decays are extremely rare due to the quadratic Glashow–Iliopoulos–Maiani (GIM) suppression and the Cabibbo suppression of the $t \to d$ transition; they can only proceed through Z penguin and W box (one-loop) diagrams. The decay amplitudes are dominated by short-distance dynamics, with the leading SM contribution generated by top-quark loops. Additionally, the $K \to \pi\nu\bar{\nu}$ decay rates are computed with negligible theoretical uncertainty, since the hadronic matrix element can be extracted from the precisely measured $K^+ \to \pi^0 e^+ \nu_e$ decay. The SM predictions for the branching ratios are $\mathcal{B}(K^+ \to \pi^+\nu\bar{\nu}) = (8.4 \pm 1.0) \times 10^{-11}$ and $\mathcal{B}(K_L \to \pi^0\nu\bar{\nu}) = (3.4 \pm 0.6) \times 10^{-11}$ [1], with uncertainties dominated by the external input parameters [2], and with more recent computations obtained in [3, 4]. The $K \to \pi\nu\bar{\nu}$ decays are therefore excellent probes of flavour physics: their strong suppression within the SM provides outstanding sensitivity to possible New Physics (NP) scenarios [5, 6]. NP models may enhance or suppress these rates through new sources of flavour violation, or introduce tree-level FCNC contributions mediated by heavy gauge bosons (Z') [7]. In such models, the combined measurement of $\mathcal{B}(K^+ \to \pi^+\nu\bar{\nu})$ and $\mathcal{B}(K_L \to \pi^0\nu\bar{\nu})$ can reveal characteristic correlations. In addition, NP models featuring Lepton Flavour Universality Violation (LFUV) [8] can link the $K^+ \to \pi^+\nu\bar{\nu}$ branching ratio to the anomalies observed in semileptonic B-meson decays, offering complementary constraints on leptoquark scenarios [9, 10].

The experimental challenge lies in detecting $K \to \pi\nu\bar{\nu}$ events among more than 10^{12} kaon decays, while controlling backgrounds from dominant two- and three-body kaon decay modes at the 10^{-11} level. The $K_L \to \pi^0\nu\bar{\nu}$ decay is currently investigated by the KOTO experiment [11]. The NA62 experiment at CERN is designed to precisely measure the $K^+ \to \pi^+\nu\bar{\nu}$ decay by exploiting a high-intensity 400 GeV/c proton beam from the SPS and a novel decay-in-flight technique [12–14]. This paper presents the NA62 observation of the $K^+ \to \pi^+\nu\bar{\nu}$ decay and the measurement of its branching ratio, based on data collected during Run 1 (2016–2018) and Run 2 (2021–2022). The result constitutes the first observation of this decay, and the smallest branching ratio measured with a signal significance above 5σ, marking a milestone in precision kaon physics [15].

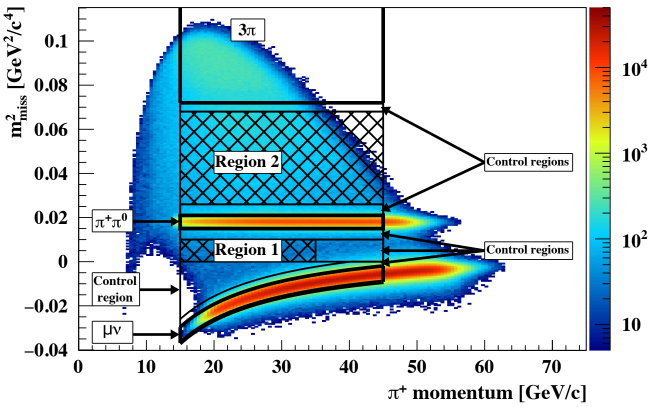

Figure 2: Distribution of the kinematic variable $m^2_{\text{miss}} = (P_K - P_\pi)^2$ versus π^+ momentum, and definition of signal (Region 1, Region 2), control and background ($\pi^+\pi^0$, $\mu\nu$, 3π) regions used in the data analysis.

2. The NA62 Experiment

NA62 is a high-precision fixed-target experiment operating in the north area of the CERN SPS. It is designed to measure $\mathcal{B}(K^+ \to \pi^+\nu\bar{\nu})$ using a decay-in-flight technique, in which 75 GeV/c kaons decay within a 60 m-long fiducial volume (FV) evacuated to $\sim 10^{-6}$ mbar. A 400 GeV/c SPS proton beam impinges on a beryllium target, producing a secondary unseparated hadron beam composed of about 6% K^+, 70% π^+ and 24% protons. The NA62 beamline and detector are described in details in [16], and were upgraded for the 2021 data taking; a sketch is shown in Figure 1. The excellent performance of this detector [17–19] is the foundation for a broad physics programme in flavour physics and beyond.

Upstream detectors Located before the FV, the upstream detector system measures and tags each incoming kaon. The KTAG is a differential Cherenkov counter providing K^+ identification with 70 ps resolution [20]. The Gigatracker (GTK) is a set of silicon-pixel tracking stations operated in vacuum, measuring the momentum, direction, and time of every incoming kaon with 0.2% momentum resolution and 100 ps timing precision. The CHANTI is a scintillator hodoscope placed downstream of the GTK serving as vetoes for beam interactions upstream of the decay region.

Fiducial decay volume The decay region extends over 60 m and is kept under high vacuum to reduce backgrounds from particle interactions with the material. A signal decay occurring within this volume is characterised by a single outgoing charged track reconstructed downstream, with no additional activity in the hermetic veto system. The FV is surrounded by photon-veto detectors that ensure a 4π coverage for photons from π^0 decays. About 5 MHz kaon decays occur within the FV.

Downstream detectors After the decay region, the daughter pion and any secondary particles are measured by a set of sub-detectors arranged along the beam axis. A Straw spectrometer made up of four vacuum straw-chamber stations, separated by a dipole magnet (270 MeV/c kick), provides a momentum resolution of $\sigma(p)/p < 0.3\%$. A RICH detector, 17 m-long neon gas counter, offers π/μ separation for 15–35 GeV/c pions and 70 ps timing [21]. A LKr electromagnetic calorimeter

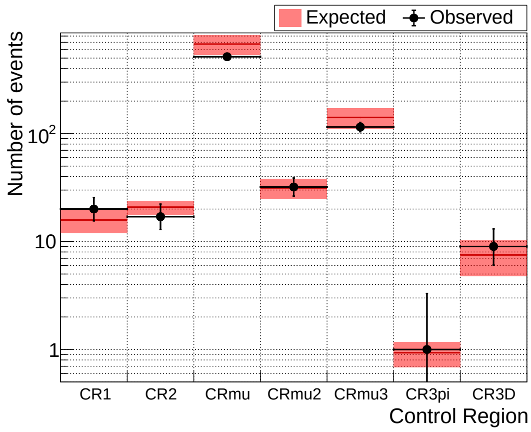

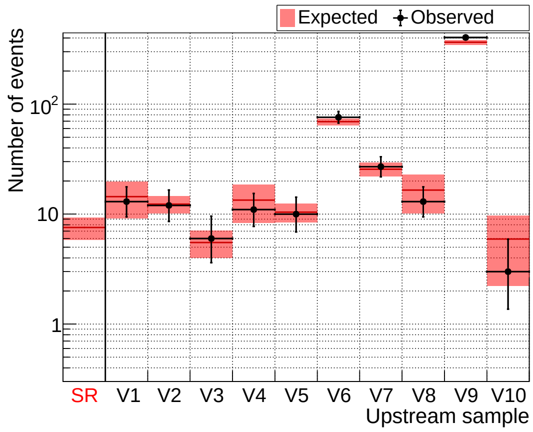

Figure 3: Validation of background in control regions. Left: expected and observed numbers of events in different control regions defined for the analysis. Right: expected and observed numbers of events in the upstream validation samples. The first bin is the signal region and therefore only the expectation is displayed.

measures electromagnetic showers and vetoes photons. MUV1-3 (muon veto) are iron/scintillator calorimeters downstream of the LKr identifying muons and rejecting $K^+ \to \mu^+\nu$ decays with a suppression factor at the level of 10^8. Large-angle photon vetoes (LAV) are 12 stations surrounding the vacuum tank, covering 8.5–50 mrad angles to achieve photon detection inefficiency below 10^{-4} for $E_\gamma > 200$ MeV. Small-angle vetoes (IRC and SAC) are located around and downstream of the beam pipe to veto forward photons escaping at small polar angles.

3. Analysis Strategy

The signature of the $K^+ \to \pi^+\nu\bar{\nu}$ decay is a single positively-charged track compatible with a pion, matched in time and direction to a tagged kaon, and accompanied by no additional activity in the detector. The analysis relies on four main pillars: kinematic constraints, particle identification, photon and multiplicity vetoing, and precise timing to ensure correct kaon-pion association. The selection is optimised in bins of pion momentum (15–45 GeV/c), where signal acceptance and background rejection are best balanced. As shown in Figure 2, the squared missing mass, $m^2_{\text{miss}} = (P_K - P_\pi)^2$ computed under the pion mass hypothesis, is used together with the pion momentum (p_{π^+}) to define two signal regions (Region1 and Region2), avoiding the kinematic peaks of the dominant kaon decay modes $K^+ \to \mu^+\nu_\mu$ and $K^+ \to \pi^+\pi^0$. Using kinematics alone provides background suppression at the level of $O(10^4)$. The branching ratio is extracted relative to the abundant normalisation mode $K^+ \to \pi^+\pi^0$, which shares the same trigger and reconstruction chain. The effective number of normalisation events is $N^{\text{eff}}_{\pi\pi} = (1.953 \pm 0.005) \times 10^8$, and the corresponding number of kaon decays in the fiducial volume is $N_K = (2.85 \pm 0.01) \times 10^{12}$, derived using the branching ratio of $K^+ \to \pi^+\pi^0$, $\pi^0 \to \gamma\gamma$ decay chain, and the normalisation selection acceptance $A_{\pi\pi} = (13.410 \pm 0.005)\%$, evaluated from simulation. The single-event sensitivity ($\mathcal{B}_{\text{SES}}$) is defined as the branching ratio corresponding to one expected signal event, and is determined from the normalisation channel and acceptance corrections. For 2021–22 data it is obtained $\mathcal{B}_{\text{SES}} = (8.48 \pm 0.29) \times 10^{-12}$. Assuming the Standard Model prediction $\mathcal{B}^{\text{SM}}_{\pi\nu\bar{\nu}} = 8.4 \times 10^{-11}$, the expected number of SM signal events is: $N^{\text{SM}}_{\pi\nu\bar{\nu}} = \mathcal{B}^{\text{SM}}_{\pi\nu\bar{\nu}}/\mathcal{B}_{\text{SES}} = 9.91 \pm 0.34$.

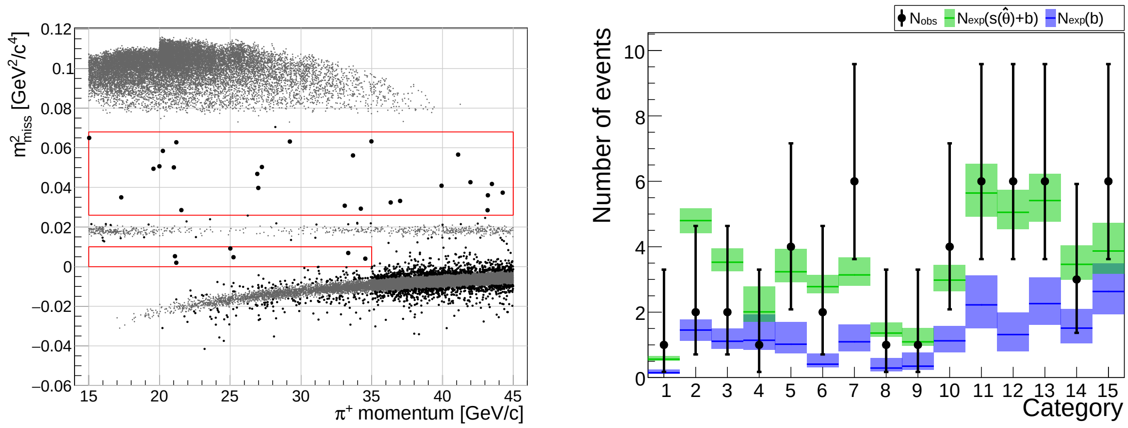

Figure 4: Left: distribution of the observed data events satisfying the signal selection criteria in the $(m^2_{\text{miss}}, p_{\pi^+})$ plane. Events in the background, control and signal regions are shown by small grey, small black and large black markers, respectively. Right: numbers of expected and observed events in the 15 categories used for the statistical analysis of 2016–2022 data. The background expectation is shown in blue, while the signal (using the measured $\mathcal{B}(K^+ \to \pi^+ \nu\bar{\nu})$) plus background expectation is shown in green.

4. Background estimation and validation

Background from $K^+ \to \mu^+ \nu(\gamma)$, $K^+ \to \pi^+\pi^0(\gamma)$ and $K^+ \to \pi^+\pi^+\pi^-$ decays in the FV arises from non-gaussian tails of the squared missing mass m^2_{miss} resolution, and is estimated from dedicated control samples. Background from $K^+ \to \pi^+\pi^- e^+ \nu$ and $K^+ \to \pi^+\gamma\gamma$ decays in the FV are estimated by using simulations. Background from early decays and interactions upstream of the FV with mismatching of the π^+ candidate, which produces a fake reconstructed vertex, is collectively referred to as "upstream" background. This is estimated with a fully data-driven strategy. Validation of the background estimates is performed by using an extensive set of statistically independent, background-enriched samples (see Figure 3). The total expected background for 2021–22 data is $N_{\text{bkg}} = 11.0^{+2.1}_{-1.9}$ events, dominated by an "upstream" background contribution of $7.4^{+2.1}_{-1.8}$ events.

5. Results and conclusions

After applying the full signal selection to the 2021–2022 dataset, a total of 31 events are found within the two predefined signal regions (see Figure 4, left). To extract the signal yield, the pion momentum spectrum is divided into six independent 5 GeV/c bins, which serve as separate statistical categories in a profile likelihood fit. The expected contributions from signal and all validated background sources are included as nuisance parameters with their uncertainties. From the fit to the 2021–2022 data alone, the branching ratio is determined to be: $\mathcal{B}(K^+ \to \pi^+ \nu\bar{\nu}) = (16.2^{+5.21}_{-4.5}) \times 10^{-11}$. These six categories are then combined with the nine categories used in the previous NA62 analysis of the 2016–2018 data [14]. The comparison of expectation (based on the measured branching ratio value) and observations across the 15 categories is summarised in the right plot of Figure 4. The combined likelihood fit over Run 1 and Run 2 statistics (2016–2022) yields:

$$\mathcal{B}(K^+ \to \pi^+ \nu\bar{\nu})_{2016-2022} = (13.0^{+3.0}_{-2.7}(\text{stat}) \pm 1.3(\text{syst})) \times 10^{-11} = (13.0^{+3.3}_{-3.0}) \times 10^{-11}$$

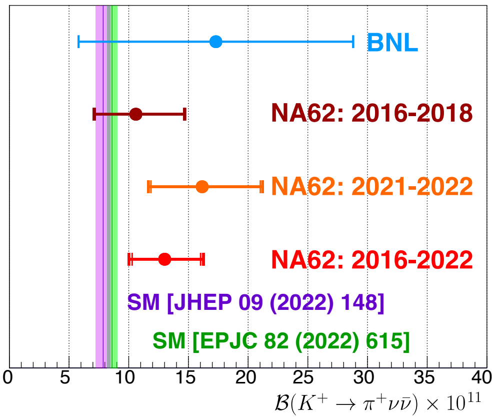

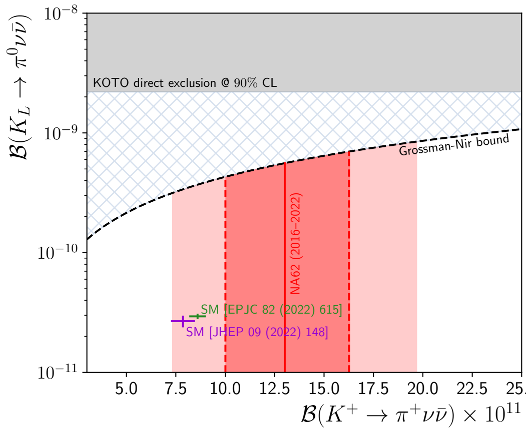

Figure 5: Left: summary of $\mathcal{B}(K^+ \to \pi^+\nu\bar{\nu})$ measurements from the BNL E787 and E949 experiments [22] and the NA62 experiment using the 2016–2018 [14], 2021–2022 and 2016–2022 [15] datasets. Statistical and total uncertainties are shown by thinner and thicker vertical bars, respectively. These are compared to the two recent SM predictions [3, 4]. Right: global status of the $K \to \pi\nu\bar{\nu}$ decay modes, showing the latest $\mathcal{B}(K_L \to \pi^0\nu\bar{\nu})$ upper limit set by the KOTO experiment [11] and the $\mathcal{B}(K^+ \to \pi^+\nu\bar{\nu})$ result from NA62 with 2016–2022 data (the 1σ and 2σ ranges are displayed in darker and lighter shaded areas, respectively).

In total, 51 events are observed in the combined dataset, compared to an expected background of 18^{+3}_{-2} events. The background-only hypothesis is rejected with $p = 2 \times 10^{-7}$, and the probability of observing such an excess corresponds to a significance greater than 5σ, constituting the first observation of the $K^+ \to \pi^+\nu\bar{\nu}$ decay. This result improves the precision on the branching ratio from approximately 40% (using 2016–2018 data alone) to around 25%, marking a major advance in the experimental exploration of rare kaon processes.

A broader comparison with previous $\mathcal{B}(K^+ \to \pi^+\nu\bar{\nu})$ measurements and the updated experimental and theoretical status is summarised in Figures 5. The NA62 measurements are self-consistent and compatible with the results from the BNL E787 and E949 experiments. The 2016–2022 NA62 result agrees with the SM predictions within 1.7σ. With further data from the 2023–2024 period currently under analysis, NA62 is expected to reach a precision at the level of 15% – 20% before LS3. Complementary studies of $K_L \to \pi^0\nu\bar{\nu}$ (at KOTO) and global fits to flavour observables will further constrain potential NP effects.

References

[1] JHEP **11** (2015) 033.
[2] Phys. Rev. D **83** (2011) 034030.
[3] Eur. Phys. J. C **82** (2022) 615.
[4] JHEP **09** (2022) 148.
[5] Eur. Phys. J. C **76** (2016) no.4 182.
[6] Eur. Phys. J. C **84** (2024) 680.
[7] JHEP **11** (2015) 166.
[8] Eur. Phys. J. C **77** (2017) no.9 618.
[9] JHEP **02** (2018) 101.
[10] Phys. Lett. B **835** (2022) 137525.
[11] Phys. Rev. Lett. **134** (2025) 081802.
[12] Phys. Lett. B **791** (2019) 156.
[13] JHEP **11** (2020) 042.
[14] JHEP **06** (2021) 093.
[15] JHEP **02** (2025) 191.
[16] JINST **12** (2017) P05025.
[17] Nucl. Instrum. Meth. A **929** (2019) 001.
[18] JHEP **03** (2023) 122.
[19] JHEP **11** (2023) 138.
[20] Nucl. Instrum. Meth. A **801** (2015) 86-94.
[21] JINST **15** (2020) P10025.
[22] Phys. Rev. D **79** (2009) 092004.

PoS(EPS-HEP2025)299